A Comparison of Delay-and-Add and Maximum Likelihood Estimation for Velocity-Selective Recording Using Multi-Electrode Cuffs

Andreis, Felipe Rettore; Metcalfe, Benjamin; Al Muhamadee Janjua, Taha; Meijs, Suzan; Favretto, Mateus Andre; Jensen, Winnie; Dos Santos Nielsen, Thomas Gomes Norgaard

Published in:
2022 44th Annual International Conference of the IEEE Engineering in Medicine & Biology Society (EMBC)

DOI (link to publication from Publisher):
10.1109/EMBC48229.2022.9870897

Publication date:
2022

Document Version
Accepted author manuscript, peer reviewed version

A Comparison of Delay-and-Add and Maximum Likelihood Estimation for Velocity-Selective Recording Using Multi-Electrode Cuffs

Felipe Rettore Andreis[1*], Benjamin Metcalfe[2], Taha Al Muhamadee Janjua[1], Suzan Meijs[1], Mateus André Favretto[3], Winnie Jensen[1], and Thomas Gomes Nørgaard dos Santos Nielsen[1]

Abstract—**Extracting information from the peripheral nervous system with implantable devices remains a significant challenge that limits the advancement of closed-loop neural prostheses. Linear electrode arrays can record neural signals with both temporal and spatial selectivity, and velocity selective recording using the delay-and-add algorithm can enable classification based on fibre type. The maximum likelihood estimation method also measures velocity and is frequently used in electromyography but has never been applied to electroneurography. Therefore, this study compares the two algorithms using in-vivo recordings of electrically evoked compound action potentials from the ulnar nerve of a pig. The performance of these algorithms was assessed using the velocity quality factor (Q-factor), computational time and the influence of the number of channels. The results show that the performance of both algorithms is significantly influenced by the number of channels in the recording array, with accuracies ranging from 77% with only two channels to 98% for 11 channels. Both algorithms were comparable in accuracy and Q-factor for all channels, with the delay-and-add having a slight advantage in the Q-factor.**

I. Introduction

Nerve cuffs are commonly used for peripheral nerve interfaces (PNIs), having been used for several decades [1]. The main advantage of cuffs over intraneural interfaces is their lower invasiveness and simplicity of surgical placement, decreasing the risk of damaging the nerve fibres and intraneural blood vessels. However, signals recorded using cuffs typically have a low signal-to-noise ratio (SNR) and thus can be severely affected by extraneural sources, such as electromyographic interference and thermal noise [2].

Several electrode configurations have been proposed to reduce the influence of external signals, such as the tripolar configuration, which was shown to reduce reflex-EMG contamination by balancing the impedances of the outer rings [3]. However, with a single tripole configuration, the energy contained in the signal is recorded by a single channel, making it challenging to differentiate between afferent and efferent signals and external noise from the nerve response. Alternatively, multiple-electrode cuffs (MECs) may be used to improve the recording capabilities of extraneural interfaces [4]. In addition to distinguishing between efferent and afferent fibres by considering the signal's direction of propagation, the MEC takes advantage of the known proportional relationship between axon diameter and action potential conduction velocity, which can be obtained by dividing the distance between electrodes by the conduction delay. Alternatively, artificially delaying the observed signals and then summing them provides maximum response when the artificial delay matches the conduction delay, i.e., a velocity-selective filter [5]. This delay-and-add approach has been validated in frogs [6], pigs [7], and rats [8] for electrically evoked compound action potentials (eCAPs) and naturally occurring neural signals in the rat dorsal rootlet [9] and pig vagus nerve [10].

Estimating conduction velocity from recordings made using arrays of electrodes has also been considered using linear [11] and two-dimensional [12] surface electrode arrays in electromyography. While for a MEC, the delay-and-add algorithm has been used, the maximum likelihood (ML) estimator is used for estimating motor unit conduction velocity in electromyography. Despite the similarities in the two domains, there have been no comparative studies on the performance of each estimation procedure. Therefore, this study compares the performance of the ML estimator with the delay-and-add algorithm for estimating the conduction velocity of electroneurographic (ENG) signals.

II. Methods

A. Surgery

All animal procedures were performed according to the Danish Veterinary and Food Administration under the Ministry of Food, Agriculture and Fisheries of Denmark (Protocol number 2017-015-0201-0137). A female Danish Landrace pig (37 kg) was anaesthetised with sevoflurane (1.5 to 2.5% minimum alveolar concentration), propofol (2

*Research supported by the European Union's Horizon 2020 research and innovation programme under the Marie Sklodowska-Curie grant agreement No 754465. The Center for Neuroplasticity and Pain is supported by the Danish National Research Foundation (DNRF121).

[1]F. R. A, T. A. M. J, S. M., W. J., and T. G. N. S. N. A. are with the Center for Neuroplasticity and Pain (CNAP), Department of Health Science and Technology, Aalborg University, Aalborg, Denmark (e-mail: fran@ hst.aau.dk).

[2]B. M. is with the Centre for Biosensors, Bioelectronics, and Biodevices (C3Bio), Department of Electronic & Electrical Engineering, University of Bath, BA2 7AY, UK.

[3]M. A. F. is with the Institute of Biomedical Engineering, Department of Electrical and Electronic Engineering, Federal University of Santa Catarina, Florianopolis, Santa Catarina, Brazil.

mg/hr/kg), fentanyl (10 µg/hr/kg) and the animal was ventilated at 15 cycles per minute. The animal was placed in a supine position, and a section of approximately 20 cm of the ulnar nerve was exposed through the anterior forelimb. The nerve was then freed from surrounding tissue for the electrode implantation. At the end of the experiment, the animal was euthanised by an overdose of pentobarbital.

B. *Electrode & Instrumentation*

Two nerve cuffs were produced according to the technique described by Haugland [13]. The tripolar stimulation cuff was 10 mm long, with an inner diameter of 1.8 mm, and a 3 mm centre-to-centre distance. The recording cuff had 14 rings with a centre-to-centre distance of 3.5 mm. The two outer rings of the recording cuff were short-circuited and used as a reference. In addition, the animal was grounded via a subcutaneous stainless-steel probe connected to the epidermis and the amplifiers. The stimulation cuff was placed distally in the forelimb and the recording cuff proximally. The distance between the two cuffs was approximately 2.5 cm. A silicon sheet was placed around the recording cuff to minimise current leakage, and the cuff was closed with ligatures.

The recording cuff was connected to an amplifier bank (CyberAmp 380, Axon Instruments Inc., Burlingame, CA, USA), with a gain of 80 dB. The bipolar signals were digitised using a PCIe-6363 and a BNC-2090 connector (National Instruments, Austin, TX, USA) with a sampling rate of 90 kSs^{-1}. The signals were bandpass filtered using a fourth-order Bessel filter with -3 dB frequency at 100 Hz and 10 kHz. The experimental setup is displayed in Fig. 1.

C. *Stimulation Paradigm*

A programmable stimulator (STG4008, Multichannel Systems, Reutlingen, Germany) was configured to produce trains of asymmetric charge-balanced rectangular biphasic pulses with amplitudes from 50 µA to 10 mA with a pulse width of 100 µs. The amplitude of the second phase was 10% of the primary phase. The inter-pulse delay was 1 s with a pseudo-random Gaussian interval with a maximum of 250 ms, and the stimulation train was repeated four times.

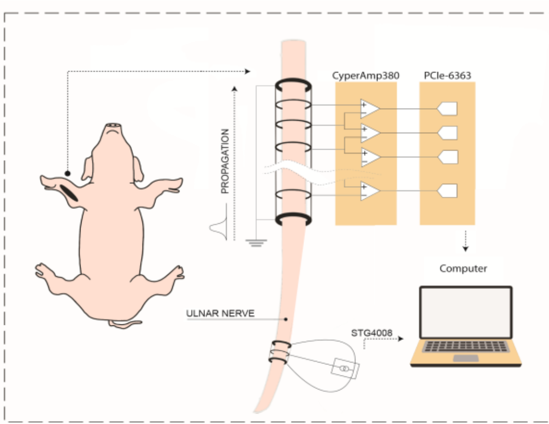

Figure 1. Experimental setup for stimulation and recording the neural signals. Tripolar cuffs were used for stimulation with the STG 4008. A 14 ring multi-electrode cuff was used to record the neural signals. The recording cuff was connected to an amplifier bank configured for bipolar recordings and digitised at a sampling rate of 90 kSs^{-1}.

D. *Data Analysis*

The time-domain ENG was segmented from -1 ms pre-stimulus to 10 ms post-stimulus. Then, each segment was further filtered using an eighth order Butterworth filter with cut-off frequencies of 300 Hz and 8 kHz. The signals were then analysed by the delay-and-add algorithm and the ML estimator.

1) *Delay-and-Add*

The delay-and-add algorithm converts the signal from the time domain into the velocity domain. The basic principle is that when using linear arrays of electrodes, each channel is delayed relative to the first channel by a time interval that depends on the signal conduction velocity and the electrode spacing. So, the delay between the first and second channel is 2*dt, the third and the first is 3*dt, and so on. This process can be formulated as

$$V_D[n, dt] = \sum_{i=1}^{C} V_{Bi}[n - (i-1) * dt] \quad (1)$$

where C is the number of channels and n is the current sample index. Consequently, by applying a range of delay values and summing the channels, the output signal will be maximal when the delay equals the quotient between the distance between the recording sites and the propagation velocity of the signal. The output signal is the intrinsic velocity spectrum (IVS). For a complete description of the delay-and-add process, see [14].

2) *Maximum Likelihood Estimator*

The ML estimator works by minimising the sum of the mean squared errors between a reference signal and the average of the other resynchronised signals. A detailed explanation can be found in [11]. In ideal conditions, K observed signals are shifted versions of a signal $s(t)$ embedded in independent white Gaussian noises $w_k(t)$ with equal variance and zero mean:

$$x_k(t) = s(t - (k-1)\emptyset) + w_k(t) \quad (2)$$
$$k = 1, \ldots, K; 0 \leq t \leq T$$

where $\emptyset$ is the delay between adjacent channels. Hence, the ML estimation of the of $\emptyset$ should minimise the error

$$e_{mle}^2 = \sum_{k=1}^{K} \sum_{n=1}^{N} [x_k(n) - s(n - (k-1)\emptyset)]^2 \quad (3)$$

where, in discrete form, N is the number of samples in an epoch of duration T. Because $s(n)$ is unknown, e_{mle}^2 is minimised with an estimate $\hat{s}(n)$ of $s(n)$

$$\hat{s}(n) = \frac{1}{K} \sum x_m(n + (m-1)\emptyset) \quad (4)$$

and replacing in (2). In the time domain, this process is limited by the sampling frequency. Therefore, the process is performed in the frequency domain, so no resolution limit is enforced [11]. In the original paper, Farina et al. proposed the iterative Newton method to detect the minimum error. As eCAPs can have multiple propagation velocities, Newton's method was not used, but the error was calculated for a vector of velocities ranging from 0.5 to 100 ms^{-1} in steps of 0.5 ms^{-1}.

3) Comparison of Algorithms

Three measures have been used to compare the algorithms. The first is accuracy: the estimated velocity compared to manually measuring the propagation velocity. The second was the velocity quality factor (Q-factor) [15], a measure of precision. As the two curves have different units (the IVS will be maximal at the matched velocity, and the ML will provide a minimum error for the matched velocity), they were normalised for displaying and comparison. The computational time required to obtain the velocity-domain signals was also measured using MATLAB running on an Intel i5-9600K CPU at 3.70 GHz, with 32 GB RAM. Finally, the influence of the number of channels was assessed. This was done by estimating the propagation velocity with only two channels and then with an increasing number of channels until it was measured across the 11 channels.

III. Results

A. Results with 11 Channels

Fig. 2 shows the eCAP response recorded with a stimulation amplitude of 2.5 mA, which resulted in a supra-threshold response. The figure shows a clear eCAP propagating from channel 1 to channel 11. While the first electrode (most distal ring) had a peak-to-peak amplitude of 627 μV, the amplitude of the last electrode was 184 μV, showing that amplitude decreased along with the electrode array. At the same time, the width of the eCAP increased. Finally, a propagation velocity of 57.14 ms^{-1} was found by manual measurement. The transformation from the time domain to the velocity domain, both for the delay-and-add and the ML estimator, is displayed in Fig. 3. The estimated conduction velocity from the delay-and-add was 56 ms^{-1} with a Q-factor of 1.89, while for the ML algorithm, the estimated velocity was 53.5 ms^{-1} with a Q-factor of 1.02. The processing time for the velocity transformation of the signals from Fig. 2 was 36.86 s and 1.06 s for the ML and the delay-and-add, respectively.

B. Influence of channel count

Accuracy, precision (Q-factor) and computational time were measured for an increasing number of channels (from 2 to 11). The accuracy increased as a function of the number of channels. The minimum accuracy was obtained for only two channels in both the ML and the delay-and-add, with values of 86.2% and 77.5%, respectively. Interestingly, the ML estimator results in a better accuracy with less than five channels, whereas the delay-and-add performs better with more than five channels. For 11 channels, the accuracy was 98.0% for the delay-and-add and 93.6% for the ML. The maximum Q-factor was observed for the delay-and-add with 11 channels (Q-factor = 1.89), whereas for 11 channels, the Q-factor of the ML estimator was 1.02. The computational time increased for both algorithms due to the number of channels. For the delay-and-add, the time ranged from 0.30 s with 2 channels to 1.06 s with 11 channels. This growth was significantly higher for the ML estimator, ranging from 0.20 s with 2 channels to 36.86 s with 11 channels. A summary of the results for 2, 6, and 11 channels is displayed in Table I.

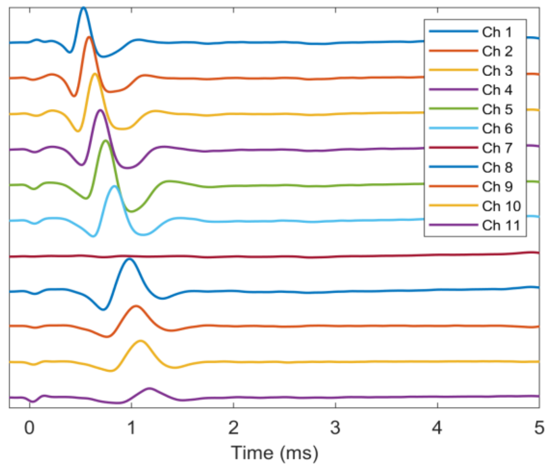

Figure 2. Time-domain recordings of the eCAP across 11 channels. An evident propagation can be seen across the channels, with decreasing amplitude and increasing width. Channel 7 was faulty, and the offset was artificially inserted for ease of visualisation. The amplitude of the first channel was 627 μV, while the last channel had an amplitude of 184 μV.

IV. Discussion

This paper has compared the ML estimator and the delay-and-add algorithm to investigate options for improving the velocity-selective recording method via a MEC placed around the ulnar nerve of a pig. Decoding information from the peripheral nervous system can be used for several purposes, such as controlling prostheses and providing sensory feedback. Moreover, classifying neural signals into fibre

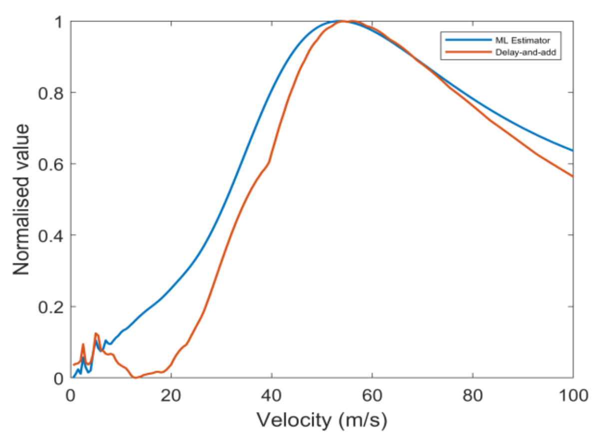

Figure 3. Velocity-domain signals. The blue line represents the results from the maximum likelihood estimator, while the orange line represents the results from delay-and-add transformation (intrinsic velocity spectra).

types can help develop closed-loop systems to target specific fibre groups when electrical stimulation is used.

TABLE I. PRECISION AND Q-FACTOR FOR THE DELAY-AND-ADD AND ML FOR 2, 6, AND 11 CHANNELS.

# of channels	**Algorithm**			
	ML		***Delay-and-add***	
	Accuracy	***Q-factor***	***Accuracy***	***Q-factor***
2	86.2%	6.5e-3	77.5%	7e-3
6	93.2%	6.6e-3	95.8%	1.21
11	93.6%	1.02	98.0%	1.89

The results suggested that the delay-and-add and the ML estimator provide similar and reasonable results for assessing conduction velocity in linear electrode arrays. The accuracy of both algorithms exceeded 90% when using 11 channels. In addition, even with only two channels, the accuracy of the ML estimator was 86%.

The ML estimator had a slightly smaller Q-factor with 11 channels, which translates directly into a reduced ability to distinguish fibre types with closer propagation velocities. The difference in the Q-factor was more pronounced between the two algorithms with decreasing number of channels. For instance, the Q-factor could not be estimated for less than 7 channels for the ML because the normalised curves (as in Fig. 3) had a slow decrease from the detected propagation velocity.

In addition, the ML estimator had a considerably higher computational time, which can be a disadvantage for real-time applications. However, this result is not unexpected, as the error was measured for a high number of delay ($\emptyset$) values (Eq. (4)). Iterative methods such as the Newton method have been proposed to improve computational efficiency [12]. However, the Newton method has not been applied in this study since eCAPs can have multiple conduction velocities, and the Newton method would provide an estimate for the minimum of the mean square error (i.e., one conduction velocity).

Having one conduction velocity is a limitation of the present data for demonstrating the effectiveness of the algorithms. Further studies are needed to investigate the performance of the algorithms in eCAPs with multiple velocities and the effect of the SNR on their classification performance.

V. CONCLUSION

This work compared the ML estimation method and the delay-and-add algorithm to estimate the conduction velocity of eCAPs recorded extraneurally using nerve cuffs. The recordings were obtained from the ulnar nerve of a pig and showed a dominant conduction velocity that was detected by both the ML estimator and the delay-and-add methods. The ML estimator had better accuracy when using less than 5 channels whereas the delay-and-add had better accuracy for more than 5 channels. For the Q-factor, the delay-and-add had slightly better results than the ML. Lastly, further analysis is necessary for eCAPs with multiple conduction velocities.

ACKNOWLEDGEMENT

The authors would like to thank the staff at Aalborg University Hospital for their assistance during the experiments.

REFERENCES

[1] R. B. Stein, T. R. Nichols, J. Jhamandas, L. Davis, and D. Charles, “Stable long-term recordings from cat peripheral nerves,” *Brain Res.*, vol. 128, no. 1, pp. 21–38, 1977, doi: 10.1016/0006-8993(77)90233-5.

[2] C. E. Larson and E. Meng, “A review for the peripheral nerve interface designer,” *J. Neurosci. Methods*, vol. 332, no. June 2019, p. 108523, 2020, doi: 10.1016/j.jneumeth.2019.108523.

[3] J. J. Struijk and M. Thomsen, “Tripolar nerve cuff recording: Stimulus artifact, EMG, and the recorded nerve signal,” *Annu. Int. Conf. IEEE Eng. Med. Biol. - Proc.*, vol. 17, no. 2, pp. 1105–1106, 1995, doi: 10.1109/iembs.1995.579534.

[4] J. T. Taylor, N. Donaldson, and J. Winter, “Multiple-electrode nerve cuffs for low-velocity and velocity-selective neural recording,” *Med. Biol. Eng. Comput.*, vol. 42, no. 5, pp. 634–643, Sep. 2004, doi: 10.1007/BF02347545.

[5] J. Taylor, M. Schuettler, C. Clarke, and N. Donaldson, “The theory of velocity selective neural recording: A study based on simulation,” *Med. Biol. Eng. Comput.*, vol. 50, no. 3, pp. 309–318, 2012, doi: 10.1007/s11517-012-0874-z.

[6] R. Rieger *et al.*, “Experimental determination of compound action potential direction and propagation velocity from multi-electrode nerve cuffs,” *Med. Eng. Phys.*, vol. 26, no. 6, pp. 531–534, 2004, doi: 10.1016/j.medengphy.2004.02.002.

[7] F. R. Andreis, B. Metcalfe, T. A. M. Janjua, W. Jensen, S. Meijs, and T. G. N. dos Santos Nielsen, “The Use of the Velocity Selective Recording Technique to Reveal the Excitation Properties of the Ulnar Nerve in Pigs,” *Sensors*, vol. 22, no. 1, p. 58, Dec. 2021, doi: 10.3390/s22010058.

[8] B. Metcalfe, D. Chew, C. Clarke, N. Donaldson, and J. Taylor, “An enhancement to velocity selective discrimination of neural recordings: Extraction of neuronal firing rates,” *2014 36th Annu. Int. Conf. IEEE Eng. Med. Biol. Soc. EMBC 2014*, no. July 2015, pp. 4111–4114, 2014, doi: 10.1109/EMBC.2014.6944528.

[9] B. W. Metcalfe, A. J. Hunter, J. E. Graham-Harper-Cater, and J. T. Taylor, “Array processing of neural signals recorded from the peripheral nervous system for the classification of action potentials,” *J. Neurosci. Methods*, vol. 347, no. October 2020, p. 108967, 2021, doi: 10.1016/j.jneumeth.2020.108967.

[10] B. W. Metcalfe, T. N. Nielsen, N. de N. Donaldson, A. J. Hunter, and J. T. Taylor, “First demonstration of velocity selective recording from the pig vagus using a nerve cuff shows respiration afferents,” *Biomed. Eng. Lett.*, vol. 8, no. 1, pp. 127–136, 2018, doi: 10.1007/s13534-017-0054-z.

[11] D. Farina, W. Muhammad, E. Fortunato, O. Meste, R. Merletti, and H. Rix, “Estimation of single motor unit conduction velocity from surface electromyogram signals detected with linear electrode arrays,” *Med. Biol. Eng. Comput.*, vol. 39, no. 2000, pp. 225–236, Mar. 2001, doi: 10.1007/bf02344807.

[12] D. Farina and R. Merletti, “Estimation of average muscle fiber conduction velocity from two-dimensional surface EMG recordings,” *J. Neurosci. Methods*, vol. 134, no. 2, pp. 199–208, 2004, doi: 10.1016/j.jneumeth.2003.12.002.

[13] M. Haugland, “Flexible method for fabrication of nerve cuff electrodes,” *Annu. Int. Conf. IEEE Eng. Med. Biol. - Proc.*, no. 1, pp. 359–360, 1996, doi: 10.1109/iembs.1996.656992.

[14] J. Taylor, B. Metcalfe, C. Clarke, D. Chew, T. Nielsen, and N. Donaldson, “A Summary of Current and New Methods in Velocity Selective Recording (VSR) of Electroneurogram (ENG),” in *2015 IEEE Computer Society Annual Symposium on VLSI*, 2015, vol. 07-10-July, pp. 221–226, doi: 10.1109/ISVLSI.2015.34.

[15] N. Donaldson, R. Rieger, M. Schuettler, and J. Taylor, “Noise and selectivity of velocity-selective multi-electrode nerve cuffs,” *Med. Biol. Eng. Comput.*, vol. 46, no. 10, pp. 1005–1018, 2008, doi: 10.1007/s11517-008-0365-4.